Crystallographic structure and magnetic ordering of UM2Al3 (M = Ni, Pd)

Alexander Krimmel, P. Fischer, B. Roessli, C. Geibel, Frank Steglich, Alois Loidl

Angaben zur Veröffentlichung / Publication details:

Krimmel, Alexander, P. Fischer, B. Roessli, C. Geibel, Frank Steglich, and Alois Loidl. 1995. "Crystallographic structure and magnetic ordering of UM2Al3 (M = Ni, Pd)." *Journal of Magnetism and Magnetic Materials* 149 (3): 380–86. https://doi.org/10.1016/0304-8853(95)00057-7.

Crystallographic structure and magnetic ordering of UM_2Al_3 (M = Ni, Pd)

A. Krimmel [a,b,*], P. Fischer [c], B. Roessli [c], C. Geibel [a], F. Steglich [a], A. Loidl [a]

[a] *Institut für Festkörperphysik, TH Darmstadt, 64289 Darmstadt, Germany*
[b] *Hahn–Meitner Institut, Glienickerstr. 100, 14109 Berlin, Germany*
[c] *Laboratory for Neutron Scattering, ETH Zürich, PSI, CH-5232 Villigen, Switzerland*

Abstract

UM_2Al_3 (M = Pd, Ni) have been studied by means of neutron diffraction experiments on polycrystalline samples. The crystallographic $PrNi_2Al_3$-type structure has been confirmed, while enormous large preferred orientation effects have been revealed. Concerning the magnetic structures, special emphasis is given to the evolution of a second incommensurate magnetic phase in UPd_2Al_3.

Neutron powder diffraction studies have been performed on UM_2Al_3 (M = Ni, Pd) on the multidetector instrument DMC at the 10 MW Saphir reactor of the PSI, Villigen, Switzerland. Most experiments were carried out in the high intensity mode using neutrons of wavelength $\lambda = 1.7008$ Å [1]. Concerning the magnetic ordering, the main results have been reported recently [2]. Here we concentrate on further results, predominantly with respect to the structures.

1. Chemical structure

Polycrystalline samples of approximately 20 g of UM_2Al_3 consisting of rather large grains have been investigated in the temperature range 1.5–300 K. The specimens were not powdered any further to avoid any possible change of their magnetic and especially of their superconducting properties. First, low-temperature neutron diffraction experiments were performed by means of an ILL-type cryostat with a fixed sample position. The diffraction patterns were analysed by the standard Rietveld refining method. Corresponding profile fits based on the hexagonal $PrNi_2Al_3$-type structure as proposed in the literature [3,4] yielded rather bad agreement values R_I concerning the integrated nuclear neutron intensities of the order of 20% for both M = Ni and Pd in the paramagnetic state. Two possible explanations could account for this behaviour. First, due to the rather large grains of the sample, preferred orientation effects could have changed the diffraction pattern. This is a well known problem in this class of compounds, as has been inferred from susceptibility and dilatation measurements with a single crystal [5]. This had to be a surprisingly large effect because it could not be corrected for by the standard preferred

* Corresponding author.

orientation calculation within the Rietveld programs. Secondly, a structural phase transition could have occurred. To clarify this point, we performed additional measurements. The coarse powder sample was mounted onto a CTI cooling machine, allowing oscillation around the vertical axis to average over different orientations of the grains. This experimental arrangement led to good agreement between calculated and measured intensities over the whole temperature range (see Fig. 1), resulting in R-values of about 4% for UPd_2Al_3 at 30 K. A high-resolution neutron diffraction study of UPd_2Al_3 at room temperature with the sample rotating around the vertical axis resulted in $R_I = 4.8\%$ without any preferred orientation correction, thus nicely confirming the $PrNi_2Al_3$-type structure (see Tables 1 and 2). A second experiment was carried out with another sample of UPd_2Al_3, this time carefully powdered to rule out any preferred orientation. Here again, the data fitted very well with the given $PrNi_2Al_3$-type structure for all temperatures used, yielding again R-values of about 4%. The corresponding variations of the lattice constants with temperature are shown in Fig. 2. Evidently, there are some differences between the two samples, but they tend to converge at low temperatures. The carefully powdered sample displays a rather drastic change (definitely outside the error bars) of the c-lattice constant while changing the temperature from 30 to 100 K. The reason for this behaviour is not clear at the moment. Similar to the case of UPd_2Al_3, the diffraction pattern of UNi_2Al_3 exhibits large preferred orientation effects. As illustrated in Fig. 3 also for UNi_2Al_3, a high-intensity neutron diffraction measurement with a rotating sample confirms the $PrNi_2Al_3$-type structure without preferred orientation correction and an agreement value of $R_I = 3.8\%$. The corresponding structural parameters are compared in Table 2 to those of UPd_2Al_3.

2. Magnetic structure

As reported recently in Ref. [2] and illustrated in Fig. 4, UPd_2Al_3 orders magnetically below 15 K, comprising a magnetic structure of ferromagnetic sheets in the easy hexagonal plane and coupled

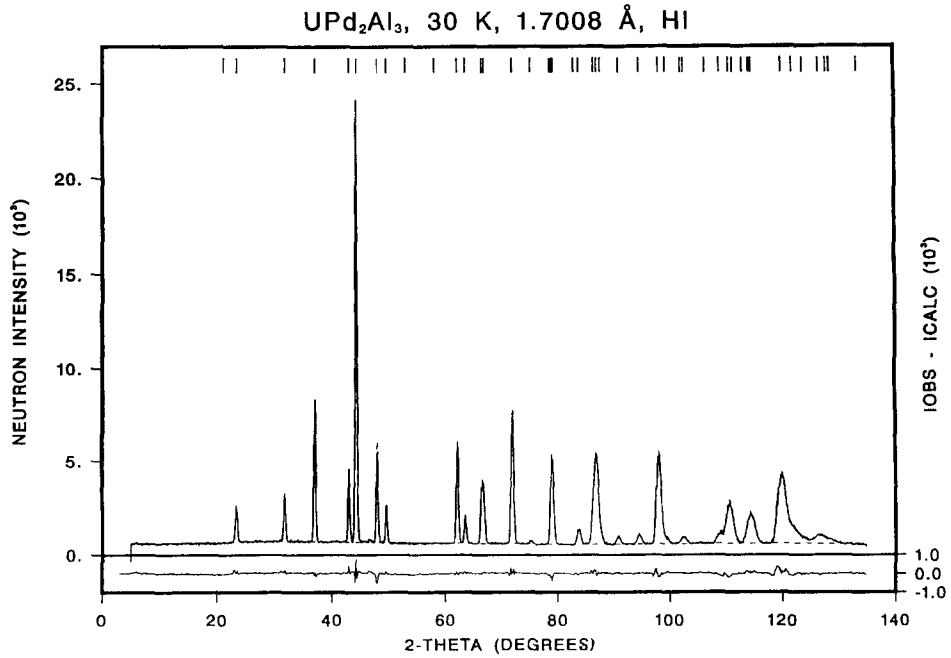

Fig. 1. Neutron powder diffraction pattern of UPd_2Al_3 at $T = 30$ K. The sample, consisting of large grains, was rotated to average over different orientations, resulting in a fit with agreement value R_I of approximately 4%. The difference between observed and calculated intensities is shown at the bottom. The vertical bars on top of the figure indicate calculated peak positions.

Table 1
Observed and calculated integrated neutron intensities of UPd_2Al_3 at $T = 295$ K for high resolution. Space group P6/mmm; U: site 1a (0 0 0); Pd: position 2c (1/3 2/3 0) and Al: site 3g (1/2 0 1/2)

h	k	l	2Θ (deg)	I_{calc}	I_{obs}
0	0	1	23.426	2285	2259
0	1	1	31.719	2767	2680
1	1	0	36.947	8202	8262
0	2	0	42.924	3628	4336
1	1	1	44.212	23335	24349
0	0	2	47.911	5594	4904
0	2	1	49.472	2027	2133
0	1	2	52.890	22	0
1	2	0	57.897	18	0
1	1	2	62.000	6562	6215
1	2	1	63.320	1620	1725
0	2	2	66.263	3440	3338
0	3	0	66.574	2434	3194
0	3	1	71.631	10380	10317
0	0	3	75.040	292	221
1	2	2	78.362	19	25
2	2	0	78.653	7554	7047
0	1	3	78.977	591	582
1	3	0	82.541	9	8
2	2	1	83.435	1533	1570
0	3	2	86.109	4146	4351
1	1	3	86.713	8090	8076
1	3	1	87.284	1053	1322
0	2	3	90.550	775	785
0	4	0	94.071	1098	1144
2	2	2	97.640	11947	12285
0	4	1	98.825	709	897
1	3	2	101.531	11	20
1	2	3	102.146	927	853
2	3	0	105.771	5	0
0	0	4	108.593	1674	1720
0	3	3	110.138	6782	6474
2	3	1	110.746	902	909
0	1	4	112.692	5	2
0	4	2	113.622	1991	2090
1	4	0	113.933	3453	3661
1	4	1	119.216	13571	13843
1	1	4	121.309	3498	3570
2	2	3	123.031	1281	1334
0	2	4	125.916	2058	1855
2	3	2	126.978	9	8
1	3	3	127.737	949	921
0	5	0	132.332	2	21

antiferromagnetically along the c-axis with an ordered magnetic moment of $0.85\mu_B$. To investigate in detail the temperature dependence of the magnetic order, the first, coarse powder sample (large grains) was mounted on the two-axis instrument P2AX at

Table 2
Structural parameters of UM_2Al_3 (M = Ni, Pd), refined by neutron powder diffraction at room temperature. Lattice parameters a,c; isotropic temperature factors B_i, neutron wavelength λ; agreement values concerning integrated intensities R_I, weighted profile factor R_{wp}, expected value R_{exp}; goodness of fit χ^2

	Pd	Ni
a (Å)	5.3688(1)	5.2193(2)
c (Å)	4.1899(1)	4.0177(2)
B_U (Å^2)	0.33(3)	0.18(6)
B_{Pd} (Å^2)	0.47(3)	0.31(4)
B_{Al} (Å^2)	0.59(4)	0.27(3)
λ (Å)	1.7012	1.7008
R_I (%)	4.6	3.8
R_{wp} (%)	7.4	6.8
R_{exp} (%)	2.1	3.0
χ^2	12.0	5.1

the Saphir reactor of the PSI. The wavelength of the incident neutron beam was 2.33 Å. On monitoring the first and strongest magnetic Bragg peak (0 0 1/2)

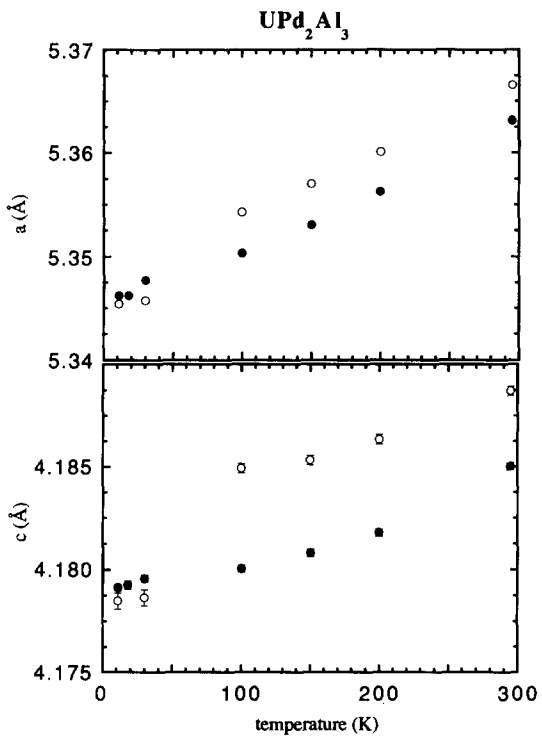

Fig. 2. Temperature dependence of the lattice constants of UPd_2Al_3 of two different samples. Full circles correspond to the coarse powder sample (large grains), open circles correspond to the fine powder sample (small grains). The error bars are either indicated or smaller than the symbol size.

with varying temperature, a second transition to an incommensurate (IC) phase has been detected on heating up the sample above 15 K. The temperature variation of this peak (0 0 1/2) is shown in Fig. 5 in the vicinity of the expected Néel temperature. It clearly documents the evolution of an IC phase out of the antiferromagnetic (AF) structure. The positions of the two principal satellites in reciprocal lattice units correspond to (0 0 0.5 ± 0.021). We have calculated the positions of the additional magnetic reflections by using a propagation vector of either (0 0 0.521) or (0 0 0.479), yielding correct Bragg angles for both cases, but with different multiplicities. $q = (0\ 0\ 0.521)$ results in two reflections $(0\ 0\ 0)^+$ and $(0\ 0\ 0)^-$ at $2\Theta = 16.7°$ compared with one reflection $(0\ 0\ 1)^-$ at 15.2°. On the other hand, $q = (0\ 0\ 0.479)$ gives $(0\ 0\ 0)^+$ and $(0\ 0\ 0)^-$ at $2\Theta = 15.2°$ leaving $(0\ 0\ 1)^-$ at 16.7°. The positive sign of the propagation vector, i.e. $q = (0\ 0\ 0.521)$ is determined by the fact that the intensity ratio of the satellites (0 0 0.5 + 0.021) to (0 0 0.5 − 0.021) in accord with their multiplicities should behave as 2 to 1; in agreement with the measurements (compare the panel of Fig. 5 at $T = 17$ K). The IC phase was determined by measuring altogether four of its magnetic Bragg peaks. Slight variations of the position of the reflections display the incommensurability. An intended Rietveld analysis to determine the magnetic structure was hampered because of the low intensities just above the sensitivity of the instrument (compare again with Fig. 5). Assuming a rather similar magnetic structure for the IC phase to that for the AF structure (for example, small distortions of the direction of the magnetic moments and not a complete spin reorientation), the magnetic intensities of the IC phase compared with the intensities of the AF phase correspond to an orthogonal component of the magnetic moment of approximately $0.2\mu_B$. This is a very large ordered magnetic moment compared with those of other known heavy-fermion superconductors, i.e. $CeCu_2Si_2$, UPt_3, UBe_{13}, URu_2Si_2. This IC phase is stable up to 20 K and coexists with the AF structure in a narrow temperature regime. The slightly larger propagation vector compared to the AF phase

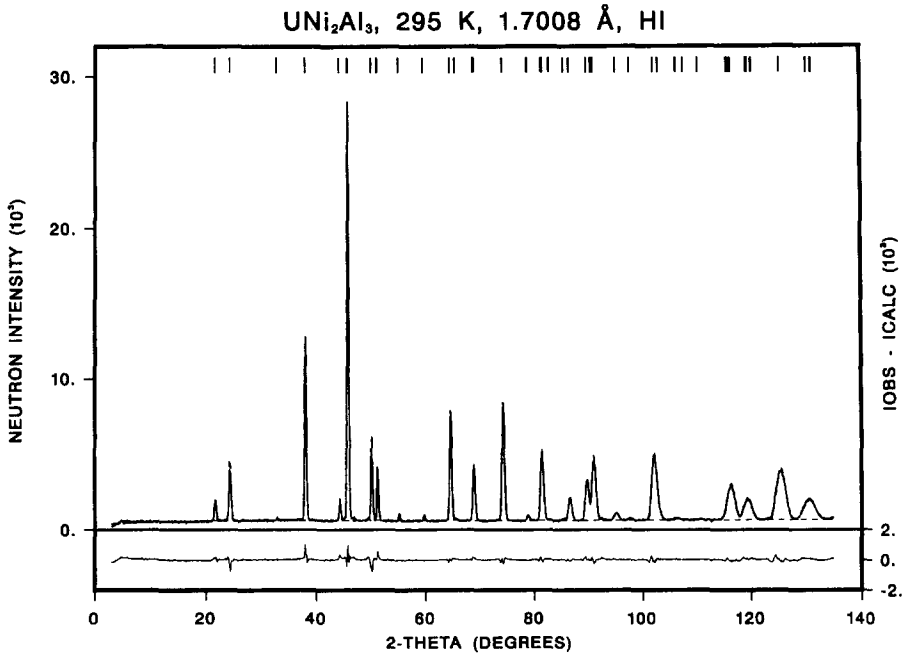

Fig. 3. Neutron powder diffraction pattern of UNi_2Al_3 at room temperature. The sample, consisting of large grains, was rotated to average over different orientations resulting in a good fit with agreement value R_I of approximately 4%. Here again, the difference between observed and calculated values is shown in the lower part and the vertical bars indicate calculated peak positions.

might just reflect the increasing disorder with increasing temperature. On cooling down again, a remarkable hysteresis effect led to an almost suppression of the IC phase. Large hysteresis effects are a common feature in systems involving transitions to incommensurate phases [6]. Cycling the temperature several times gave reproducible results.

So far, there is no unambiguous confirmation of this IC structure. In particular, first neutron diffraction studies on single-crystalline material could not detect any additional magnetic phase [7], nor did other measurements [8]. However, very recent experiments seem to indicate the presence of weak magnetic Bragg peaks belonging to an IC structure [9].

It is very interesting to compare the situation of UPd_2Al_3 with its cerium homologue. The heavy-fermion system $CePd_2Al_3$ also crystallizes in the hexagonal $PrNi_2Al_3$-type structure. Below $T_N = 2.9$ K it displays the same type of AF ordering as UPd_2Al_3, but it does not become superconducting. Early neutron diffraction studies on polycrystalline $CePd_2Al_3$ claimed the existence of an IC magnetic structure just above $T = 2.9$ K [10]. In contrast, single-crystal experiments could not find indications of any magnetic order at all. As pointed out in Ref. [11], the physical properties of $CePd_2Al_3$ are very sensitive to sample preparation conditions. Site disorder and vacancies can easily destroy long-range magnetic order. A more recent and very detailed neutron scattering study on high-quality polycrystalline samples [12] confirmed the AF ordering at low temperatures without giving evidence for any IC structure in $CePd_2Al_3$. But there are two important differences compared to UPd_2Al_3. First, based on the intensity peak-to-background ratios, the IC structure in UPd_2Al_3 is much more significant than it is in $CePd_2Al_3$. Second, and in sharp contrast with the Ce compound, polycrystalline UPd_2Al_3 is of higher crystallographic quality than single crystals. This fact is most pronounced by the superconducting transi-

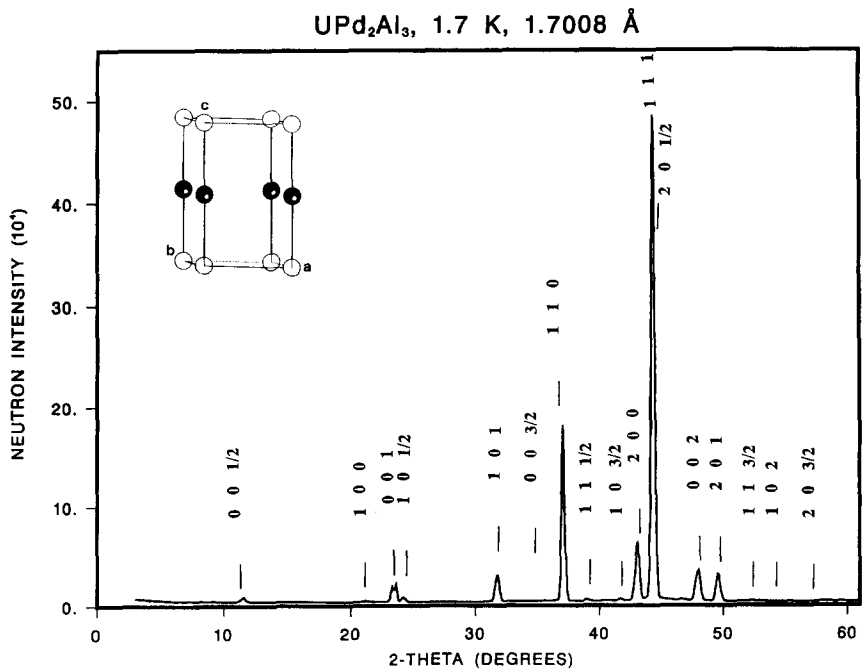

Fig. 4. Neutron powder diffraction pattern of UPd_2Al_3 in the magnetically ordered state at $T = 1.7$ K. Both, the nuclear as well as the magnetic Bragg peaks can be indexed unambiguously assuming the $PrNi_2Al_3$-type nuclear structure and a magnetic structure as illustrated in the inset: ferromagnetic sheets in the easy hexagonal plane (full and open circles respectively) coupled antiferromagnetically along the c-axis with an ordered moment of $0.85\mu_B$. For clarity, only the uranium ions of one unit cell are shown. The calculated peak positions are indicated at the top of the figure.

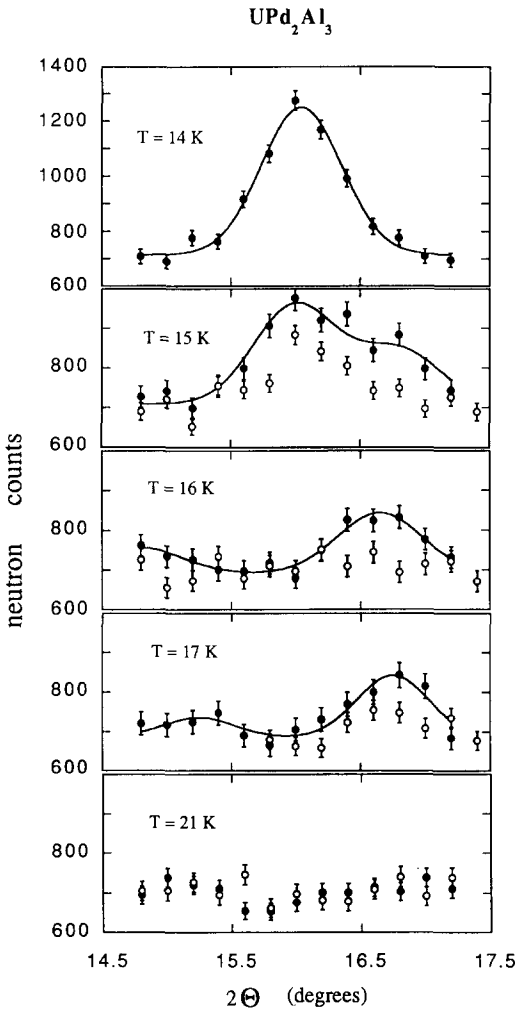

Fig. 5. Temperature dependence of the magnetic intensities in the vicinity of the antiferromagnetic phase transition. For $T = 14$ K ($T < T_N$), there is a well defined magnetic Bragg peak (0 0 1/2) of the AF structure as described above and in Ref. [2]. For $T = 15$ K, slightly above the Néel temperature found by bulk measurements, the dominant magnetic Bragg peak (0 0 1/2) is still fully developed, but additional satellites are appearing. Heating further up to 16 K, now the AF structure has vanished completely, just leaving magnetic intensity corresponding to an incommensurate structure. Going up to 17 K, we are left with two magnetic peaks which can be indexed by a propagation vector $q = (0, 0, 0.521)$. At $T = 21$ K, a reasonable fit is no longer possible. Full and open circles correspond to heating and cooling cycles, respectively. The intensity is always lower when cooling rather than heating the sample.

tion temperatures that are usually higher in polycrystalline material, and its widths ($\Delta T_c \approx 20$–50 and 100–200 mK for polycrystalline and single-crystalline samples, respectively). This last point is a further argument that the IC structure of UPd_2Al_3 is an intrinsic property of the compound.

Concerning UNi_2Al_3, our neutron diffraction data could not detect any magnetic ordering. Taking into account the sensitivity of the instrument, an upper limit of the ordered moment of $\mu \leq 0.2\mu_B$ could be estimated. Recently, a neutron scattering study using a single crystal [13] revealed an IC magnetic structure with an ordered magnetic moment of $\mu = (0.24 \pm 0.1)\mu_B$ coexisting with the superconducting state. These findings give further support for the occurrence of an IC structure in UPd_2Al_3.

To conclude, the magnetic (and superconducting) properties of UPd_2Al_3 and its homologues seem to be critically dependent on the sample preparation procedures. The (heavy-fermion) compounds of this structure type tend to a certain extent to the formation of an incommensurate magnetic structure. This may be related to its other unusual physical properties in the future.

References

[1] J. Schefer, P. Fischer, H. Heer, A. Isacson, M. Koch and R. Thut, Nucl. Instrum. Meth. Phys. Res. A288 (1990) 477.

[2] A. Krimmel, P. Fischer, B. Roessli, H. Maletta, C. Geibel, C. Schank, A. Grauel, A. Loidl and F. Steglich, Z. Phys. B: Condens. Matter 86 (1992) 161.

[3] C. Geibel, C. Schank, S. Thies, H. Kitazawa, C. Bredl, A. Böhm, M. Rau, A. Grauel, R. Caspary, R. Helfreich, U. Ahlheim, G. Weber and F. Steglich, Z. Phys. B: Condens. Matter 84 (1991) 1.

[4] E. Parthé and B. Chabot in: Handbook on the Physics and Chemistry of Rare Earths, eds. K.A. Gschneidner Jr., L. Eyring, Vol. 6 (North-Holland, Amsterdam, 1984), p. 235.

[5] C. Geibel, U. Ahlheim, C.D. Bredl, J. Diehl, A. Grauel, R. Helfreich, H. Kitazawa, R. Köhler, R. Modler, M. Lang, C. Schank, S. Thies, F. Steglich, N. Sato and T. Komatsubara, Physica C 185–189 (1991) 2651.

[6] P. Bak, Rep. Prog. Phys. 45 (1982) 587.

[7] A. Krimmel, P. Fischer, B. Roessli, A. Dönni, H. Kita, N. Sato, Y. Endoh, T. Komatsubara, C. Geibel, F. Steglich and A. Loidl, Solid State Commun. 87 (1993) 829.
L. Paolasini, J.A. Paixão, G.H. Lander, P. Burlet, N. Sato and T. Komatsubara, Phys. Rev. B 49 (1994) 7072.

[8] A. Amato, R. Feyerherm, F.N. Gygax, A. Schenk, M. Weber, R. Caspary, P. Hellmann, C. Schank, C. Geibel, F. Steglich, D.E. MacLaughlin, E.A. Knetsch and R.H. Heffner, Europhys. Lett. 19 (1992) 127.

[9] H. Kita, A. Dönni, Y. Endoh, K. Kakurai, N. Sato and T. Komatsubara, J. Phys. Soc. Jpn. 63 (1994) 726.

[10] S. Mitsuda, T. Wada, K. Hosoya, H. Yoshizawa and H. Kitazawa, J. Phys. Soc. Jpn. 61 (1992) 4667.

[11] S.A.M. Mentik, N.M. Bos, G.J. Nieuwenhuys, A. Drost, E. Frikkee, L. T. Tai, A.A. Menowsky and J.A. Mydosh, Physica B 186–188 (1993) 497.

[12] A. Dönni, P. Fischer, B. Roessli and H. Kitazawa, Z. Phys. B 93 (1994) 449.

[13] A. Schröder, J.G. Lusier, B.D. Gaulin, J.D. Garrett, W.J.L. Buyers, L. Rebelsky and S.M. Shapiro, Phys. Rev. Lett. 72 (1994) 136.